Separation of contributions to spin valve interlayer exchange coupling field by temperature dependent coupling field measurements

Chih-Ling Lee,[a] James A. Bain, Shaoyan Chu, and Michael E. McHenry
Department of Materials Science and Engineering, Data Storage Systems Center, Carnegie Mellon University, Pittsburgh, Pennsylvania 15213

In this work, interlayer exchange coupling fields of spin valve samples have been measured as a function of temperature, and fit to a temperature dependent combination of RKKY and Neel coupling fields. The RKKY coupling strength is assumed proportional to the form $(T/T_0)/\sinh(T/T_0)$, where T is temperature and T_0 is characteristic temperature. [N. Persat and A. Dinia, Phys. Rev. B **56**, 2676 (1997)] This allows the RKKY coupling and Neel coupling field to be separated quantitatively. The results of such an analysis on various CoFe/Cu/CoFe spin valve structures allow the extraction of a roughness parameter from the Neel model and the T_0 parameter from the RKKY model. The measured roughness on the top surface was generally 2–3 times greater than the value obtained from the Neel analysis. The extracted T_0 parameter was one order of magnitude smaller than that measured for bulk Cu by the de Hass–van Alphen effect. [N. Persat and A. Dinia, Phys. Rev. B. **56**, 2676 (1997); B. Lengeler and W. R. Wampler, Phys. Rev. B **15**, 5493 (1977)] Part of this reduction may be due to the 2D nature of the electron gas, as justified by an estimate of the 2D free electron Fermi energy calculation. However a factor of four difference remains, with the experimental value of T_0 being around 100 K. This behavior, while not fully explained, is consistent with the measurements of other workers. © *2002 American Institute of Physics.* [DOI: 10.1063/1.1451598]

I. INTRODUCTION

For a number of years, researchers[1–3] have studied the interlayer coupling behavior of two ferromagnets that are separated by a nonmagnetic spacer. The main interlayer coupling effects have been identified to be RKKY-like coupling[4–6] (an indirect exchange mediated by the electrons in the spacer), Neel's orange peel coupling[7] (a topological magnetostatic effect), and direct exchange through pin hole coupling.[8] In order to quantitatively separate the coupling effects, studies have been performed in which the thickness of the nonmagnetic spacer was changed to examine different interlayer coupling fields.[9–12] Kools and Leal have reported on the separation of RKKY-like and Neel's coupling by using a linear combination of these two energies to fit the total coupling energy versus spacer thickness.

Besides changing the nonmagnetic spacer thickness, another approach for separating these two factors is discussed in this paper. This method involves the measurement of the temperature dependent interlayer exchange coupling field. It assumes that the Fermi velocity of the electrons, ν_F, at the extreme points of the spacer Fermi surface affects the extent of temperature dependence of the exchange energy. The one-electron model[13] and the free electron model[14–15] both predict the exchange coupling strength, J, to have the following temperature dependence $J(T)$:[16,17]

$$J(T)=J_0\frac{T/T_0}{\sinh(T/T_0)}, \tag{1}$$

where J_0 is the coupling strength at 0 K, and T_0 is a characteristic temperature given by

$$T_0=\frac{\hbar\nu_F}{2\pi\kappa_B t_s}. \tag{2}$$

In Eq. (2), t_S is the nonmagnetic spacer thickness and ν_F is the Fermi velocity of the relevant electrons in the spacer.

The interlayer exchange coupling field in this work is assumed to consist only of RKKY-like coupling and Neel's orange peel coupling. In other words, the total coupling energy,[11,12] E_{total}, can be expressed as

$$E_{\text{total}}=E_{\text{ex}}+E_{\text{topo}}, \tag{3}$$

where the E_{ex} is the oscillatory RKKY exchange interaction for the free layer and E_{topo} is Neel-type topological coupling energy. Following Eq. (1) above, the full RKKY term, E_{ex}, is expressed by the following relationship:[9–12]

$$E_{\text{ex}}=\frac{E_0}{(k_0 t_s)^2}\sin\left(\frac{2\pi t_s}{\Lambda}+\psi\right)\frac{T/T_0}{\sinh(T/T_0)}, \tag{4}$$

where E_0 is coupling energy, k_0 is wave number, Λ is the wavelength of the coupling repeating pattern, and ψ is a phase shift.

The topological coupling term, E_{topo} can be expressed by

$$E_{\text{topo}}=\frac{\pi^2}{\sqrt{2}}\frac{\gamma^2}{\lambda}M_P M_F\exp\left(\frac{-2\pi\sqrt{2}t_s}{\lambda}\right), \tag{5}$$

where γ is the waviness amplitude of each film (peak-to-peak),[18] λ is the in-plane wavelength of the surface variations, and M_p and M_F are the magnetization of the pinned layer and the free layer, respectively. Therefore, the total coupling field, H_{int}, can be expressed as[12]

$$H_{\text{int}}=\frac{E_{\text{ex}}+E_{\text{topo}}}{M_F t_F}, \tag{6}$$

[a]Electronic mail: zlee@andrew.cmu.edu

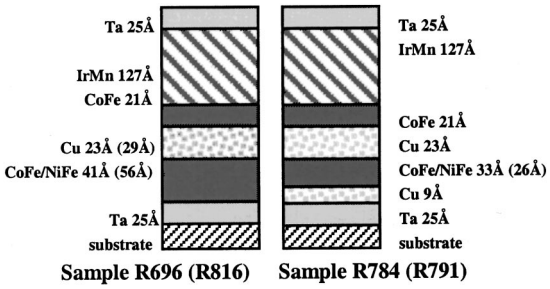

FIG. 1. Spin valve sheet films with four different structures. Sample R696 and sample R816 have same structure but different thickness of Cu and free layer. Sample R784 and sample R791 have different free layer thickness.

where t_F is the thickness of the free layer. Combining these equations gives an expression for H_{int} of

$$H_{\text{int}} = AM_P(T) + \frac{B}{M_F(T)} \frac{CT}{\sinh(CT)}, \tag{7}$$

$$\text{where } A = \frac{\pi^2}{\sqrt{2}} \frac{\gamma^2}{\lambda} \frac{1}{t_F} \exp\left(\frac{-2\pi\sqrt{2}t_s}{\lambda}\right),$$

$$B = \frac{E_0}{t_F (k_0 t_s)^2} \sin\left(\frac{2\pi t_s}{\Lambda} + \psi\right), \text{ and } C = \frac{1}{T_0}.$$

M_P and M_F are also a function of temperature. In this work, the experimental results have been fit with Eq. (7) as a function of temperature, and the parameters *A*, *B*, and *C* extracted as fitting parameters. Thus, the interlayer exchange coupling field (contained in *B* and *C*) can be distinguished from the topographic coupling field (contained in *A*).

II. EXPERIMENT

A series of the NiFe–CoFe/Cu/CoFe spin valve sheet films have been deposited on glass having the structures and sample IDs shown in Fig. 1. Those samples were made by a home-built dc magnetron sputtering system, which has five target positions and a base pressure below 2×10^{-7} Torr. A uniaxial in-plane magnetic field of 30 Oe was applied during deposition. The interlayer coupling field, H_{int}, was determined by the shift of the center of hysteresis loop from resistance versus magnetic field measurement. Samples were cut into 5 mm×5 mm squares for analysis. The resistance versus field measurements were done by a Physical Property Measurement System Model 6000 with the four-point contact method. A SQUID was used to measure magnetic moment vs field. Both systems were made by Quantum Design Co., and examined temperature ranges from 5 to 320 K. The contact regions for resistance measurements were sputtered Au with a thickness of 70 nm.

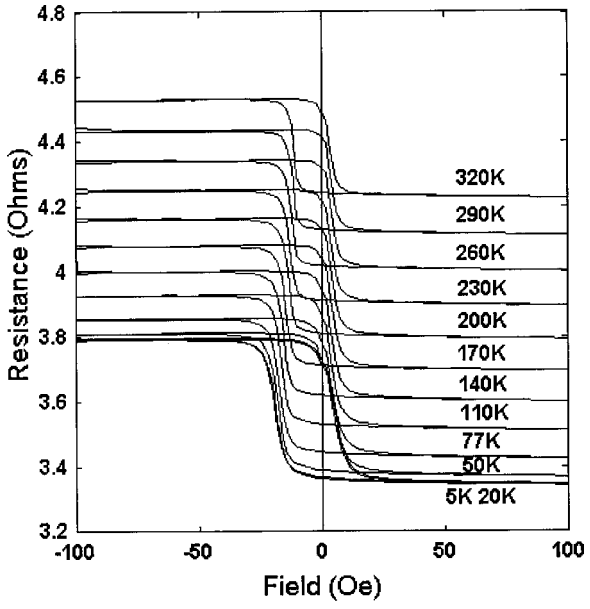

FIG. 2. Resistance vs field for sample R696. The measurement is from 320 to 5 K.

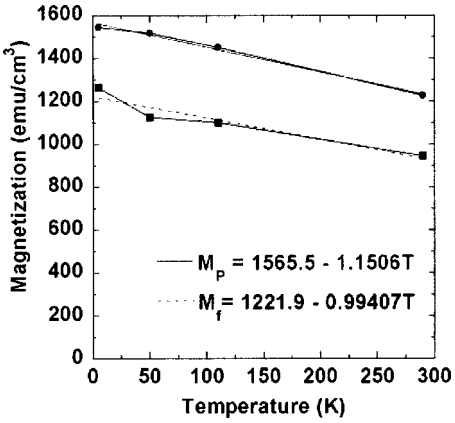

FIG. 3. Magnetization of the pinned layer and the free layer vs temperature. The measurement is from 320 to 5 K.

III. RESULTS AND DISCUSSIONS

Typical resistance versus magnetic field results are shown in Fig. 2 for one of the samples (R696). The resistance decreases as the temperature decreases as expected. The interlayer exchange coupling field (H_{int}) increases when the temperature decreased, also as expected from Eq. (7). Figure 2 also reveals that there is ferromagnetic coupling at zero field due to the low resistance state observed. The value of H_{int} was obtained in this way for all of the samples and fit with Eq. (7).

Figure 3 shows M_P and M_F as function of temperature for sample R696. The linear fitting is also shown for their magnetization degradation with temperature. Therefore, Eq. (7) can be modified as

$$H_{\text{int}} = A(1565.5 - 1.15T) + \frac{B}{1221.9 - 0.994T} \frac{CT}{\sinh(CT)}. \tag{8}$$

Figure 4 shows the result of this fitting. The circles are the experimental data and the dashed lines are the fitting curves. The results for all four samples are shown in Table I. According to Eq. (8), parameter $AM_P(0)$ is the Neel coupling field and parameter $B/M_F(0)$ is the RKKY-like coupling field at 0 K.

Several of the expressions above have been used to convert the data in Table I into a more meaningful form. These

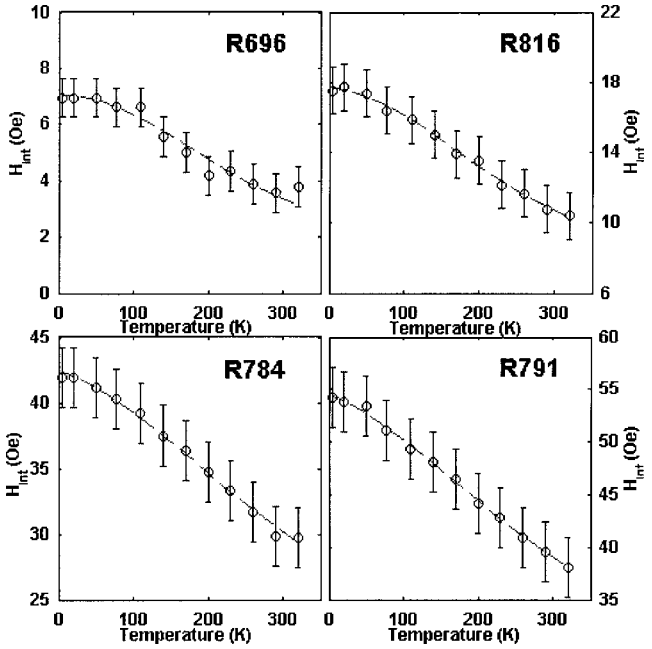

FIG. 4. Fitting results for all of samples. The circles are the experimental results. The dash line is the fitting curve.

results are shown in Table II. The coupling energies from the fitting results in the table are similar to that in previous reports of Kools[9] and Leal.[11] Some authors have reported that saturation magnetization changed with temperature in Co/Cu multilayer systems.[17] The magnetization of the pinned and the free layer exhibit a linear decreasing with temperature from SQUID measurement in this temperature range. Significantly, the T_0 from this fitting agrees with the previous report from Persat,[16] which indicated that T_0 is of the order of 100 K. The Fermi velocity of Cu indicated by these results is ten times smaller than the theoretical prediction of the free electron model for Cu of 1.57×10^6 m/s.[19] Even if a 2D free electron model is used, a Fermi velocity of 6×10^5 m/s is obtained, which is still 3–4 times larger than the observed results. Persat[1] noted that even the more precise experimental determination of the Fermi velocity at the appropriate points on the Fermi surface has not been able to explain this temperature dependence. He suggested that this behavior is determined not only by the spacer Fermi surface, but also by the ferromagnet.

By using Eq. (5), the interface roughness γ can be calculated from the fitting parameter A, with $M_p(0)$ from

TABLE I. The fitted results for all samples. The fitting parameters are based on formula (7).

	R696	R816	R784	R791
$AM_P(0)$	2.35	11.12	35.07	47.12
$B/M_F(0)$	4.67	6.53	7.365	7.365
C	0.0109	0.0113	0.0102	0.0113

TABLE II. Converted results from Table I.

	R696	R816	R784	R791
E_{topo}(erg/cm^2)	0.0012	0.0088	0.0141	0.015
E_{RKKY}(erg/cm^2)	0.0023	0.0052	0.003	0.0023
T_0(K)	92	89	98	89
V_F(m/sec)	1.74×10^5	2.11×10^5	1.85×10^5	1.67×10^5
γ (Å)	3.6 ± 0.3	9.9 ± 0.5	12.3 ± 0.6	12.6 ± 0.7
AFM (Å)	16.9	18.6	19.3	27.3

SQUID measurements. The M_p versus temperature has been shown in Figure 3. It decreases around 20% from 5 to 290 K. The λ was measured to be 120 ± 20 nm by atomic force microscopy (AFM). The AFM measurements measured the top surface of the film. Therefore, the wavelength λ, and the roughness γ, are the same at the top surface as at the interface. The roughness measurements quoted are peak to peak values.[17] The observed peak-to-peak results are consistently about 2–4 times larger than the fitted results as shown in Table II. This suggests that the IrMn is adding a consistent amount of roughness to the top surface. In addition, in a spin filter spin valve with an additional thin Cu underlayer structure, the interlayer roughness is larger than for a conventional spin valve from Table II.

IV. CONCLUSIONS

The Neel coupling and the RKKY-like coupling can be separated by fitting the experimental results with formula (7). These results agree with the previous reports. However, the low characteristic temperature and low Fermi velocity of Cu is still an open question, showing a disagreement between the observed results and theoretical calculations. The interface roughness has been calculated from the fitting results using Neel's formula. Compared to the AFM measurements at the top surface of the film, the interface roughness from the fitting results shows the same trend. However, the observed results suggest an interface three times smoother than the measured top surface of the spin valve.

[1] B. Dieny, *et al.*, J. Appl. Phys. **69**, 4774 (1991).
[2] S. S. S. Parkin *et al.*, Phys. Rev. Lett. **64**, 2304 (1990).
[3] J. Mathon, Contemp. Phys. **32**, 143 (1991).
[4] M. A. Ruderman and C. Kittel, Phys. Rev. **96**, 99 (1954).
[5] T. Kasuya, Prog. Theor. Phys. **16**, 45 (1956).
[6] K. Yosida, Phys. Rev. **106**, 893 (1957).
[7] L. Neel, C.R. Acad. Sci. **255**, 1676 (1962).
[8] Th. G. S. M. Rijks *et al.*, J. Appl. Phys. **76**, 1092 (1994).
[9] J. C. S. Kools, *et al.*, IEEE Trans. Magn. **31**, 3918 (1995).
[10] J. L. Leal and M. H. Kryder, J. Appl. Phys. **79**, 2801 (1996).
[11] J. L. Leal and M. H. Kryder, IEEE Trans. Magn. **32**, 4642 (1996).
[12] E. M. Williams, *Design and Analysis of Magnetoresistive Recording Heads* (Wiley, New York, 2001), p. 177.
[13] D. M. Edwards *et al.*, Phys. Rev. Lett. **67**, 493 (1991).
[14] P. Bruno and C. Chappert, Phys. Rev. Lett. **67**, 1602 (1991).
[15] P. Bruno and C. Chappert, Phys. Rev. B **46**, 261 (1992).
[16] N. Persat and A. Dinia, Phys. Rev. B **56**, 2676 (1997).
[17] C. Christides, J. Appl. Phys. **88**, 3552 (2000).
[18] J. C. S. Kools and W. Kula, J. Appl. Phys. **85**, 4466 (1999).
[19] B. Lengeler and W. R. Wampler, Phys. Rev. B **15**, 5493 (1977).